N73-10134

30. Prediction and Analysis of Human Performance in a VTOL Hover Task*

SHELDON BARON AND DAVID L. KLEINMAN

Bolt Beranek and Newman Inc.

An optimal control model is used to predict pilot performance in a series of longitudinal hovering tasks. Configurational changes are considered that alter significantly the system response to both control and disturbance inputs. Model predictions of mean-squared performance are compared with measurements obtained in an independent experimental study of the task. In addition, the optimal control model is used to predict describing functions that correspond to the "loop closing" pilot transfer functions frequently employed in classical multiloop manual control analyses.

INTRODUCTION

Modern control theory with its emphasis on state-space techniques and digital computation has provided the basis for systematic analysis and synthesis of multi-input, multi-output systems. In recent years this theory has been blended with results from human response theory to develop a computerized procedure for analyzing manned-vehicle systems (refs. 1 and 2). Central to this approach is an "optimal-control" or "state-variable" model of the human operator. This model has proven to be very successful in predicting human control characteristics and system performance in a variety of single-axis tracking tasks. It has also been used to analyze longitudinal hover control of an XV–5A (ref. 3). In that study, semi-empirical techniques, involving a fairly extensive preliminary experimental program, were used to determine the parameters of the optimal-control model. Using these parameters, human performance in the hover task was predicted and compared with data from simulation experiments. The results showed that the model was capable of reproducing both the correlated and uncorrelated portions of the pilot's control spectra as well as closed-loop system performance. The effects of visual scanning and a change in displayed information were also predicted.

In this paper, we also analyze longitudinal hover control. However, our emphasis is on the ability of the model to predict the effects on performance of a variety of configurational changes (i.e., changes in aircraft stability derivatives). In addition, we shall use the optimal-control model to predict describing functions that correspond to "loop-closing" pilot transfer functions that are frequently employed in classical multiloop manual control analyses.

MODEL FOR THE HUMAN OPERATOR

The optimal-control model of the human operator is predicated on the assumption that he behaves optimally subject to his inherent limitations and his understanding of the requirements of the task. This implies a *normative* approach to developing the model, i.e., we seek to determine what the human should do given his limitations and the task. This leads to a model for the pilot that has as its key elements representations of his limitations and of his compensating "processes." The resulting model has been described in detail in references 1 through 3, so we will only review briefly its basic features.

The structure of the model for the human

* This work was performed for NASA-Electronics Research Center under contract NAS12–104, and is described in greater detail in reference 1.

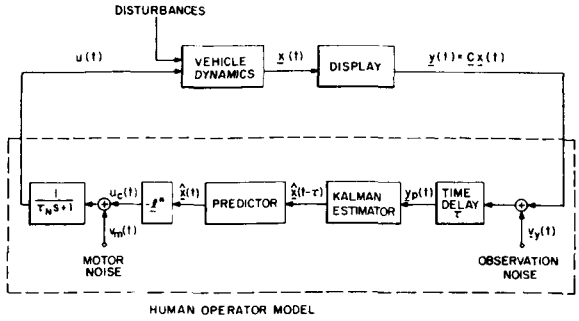

FIGURE 1.—Control theoretic model of optimal human behavior.

operator is shown in figure 1. Also shown is the model of the vehicle-display system. Vehicle dynamics are assumed to be linear and time-invariant.* The state of the vehicle is given by the vector $\underline{x}$ and the displayed variables, $\underline{y}$, are assumed to be linear combinations of the states. Input disturbances are modelled as zero-mean, gaussian, white noises passed through appropriate linear filters.†

Figure 1 illustrates several types of pilot limitations that are represented explicitly in the model. The various internal delays associated with visual, central processing and neuro-motor pathways are modelled, for convenience, by a lumped perceptual delay τ. The "equivalent" observation noise process indicated in figure 1 accounts for the effects of sensory and central processing sources of human randomness. A white, gaussian noise is added to each "observed" variable. The power density level of this noise is assumed to scale with the mean-squared value of the "signal" being observed. The noise-to-signal ratio is a parameter of the model that is expected to depend on the nature (quality, type, form) of the display. The model also includes a "motor-noise" to account for the fact that the human operator cannot generate intended control inputs perfectly. The motor noise is also assumed to be a white gaussian noise and its power density is scaled with the intended or "commanded" control u_c indicated in figure 1. The motor noise and the observation noises together account for human randomness; for situations in which quasilinear, frequency domain representations of the human are appropriate, these noises constitute a model for controller remnant.

Given the above "human" limitations, and our basic assumption, the model of the human operator then includes for "equalization": a Kalman estimator to compensate for the observation noises; a least mean-squared predictor to compensate for the time-delay; and, a set of feedback gains that are optimal in terms of minimizing a quadratic cost functional of the form

$$J=\sum_{i=1}^{n} q_i\overline{x_i^2}+g\overline{\dot{u}^2}. \qquad (1)$$

This quadratic performance index is a natural extension of the mean-squared tracking error criterion of classical compensatory tracking experiments. The cost functional weightings, $q_i \geq 0$ and $g>0$, may be either objective (specified by the experimenter or designer) or subjective (adopted by the human in performing and relating to the task). The inclusion in equation (1) of a term proportional to mean-squared control rate is an important feature of the model. This term may be thought of as constituting a subjective penalty on too rapid control movements or as an indirect method for accounting for physiological limitations on the human's bandwidth. Its inclusion results in the first order controller lag (time constant $=\tau_N$) shown in figure 1.

To apply the model, we must specify the values of its parameters: the time delay τ; the noise-to-signal ratios of the observation noises ρ_i and the motor-noise ρ_m; and the cost-functional weightings q_i, g. Our studies of single-axis control tasks have revealed a consistency of parameter values that is very encouraging. In particular, we have found that for k, k/s, and k/s^2 tracking, excellent agreement between model and measured data is obtained with the following parameter values: $\tau=0.15$ to 0.2 sec; $\rho_i \simeq 0.01$ (-20 dB); $\rho_m \simeq -0.003$ (-25 dB); $\tau_N=0.08$ to 0.1 sec. (ref. 2).

THE HOVERING TASK

The results of an analytic and experimental investigation of precision hover control by Vinje

* The time-invariance assumption is not essential for using the model to predict performance; certain "memoryless" nonlinearities can also be considered (ref. 4).

† Nonrandom inputs can also be considered (ref. 4).

and Miller (refs. 5 and 6) will provide the basic data for our investigation. They conducted a series of simulator experiments in which they measured the effects of variations in aircraft stability parameters on rms hovering performance.

Briefly, the pilot's task was to minimize longitudinal position errors while hovering in turbulent air. Only longitudinal motions were considered and the pilot was not required to control the height of the aircraft. The linearized equations used to simulate this task were

$$\left.\begin{aligned}\dot{q} &= M_u(u+u_g)+M_q q+M_\delta\delta\\ \dot{u} &= X_u(u+u_g)+g\theta\end{aligned}\right\} \qquad (2)$$

where $u=\dot{x}$ is the perturbation velocity along the x-body axis, u_g is the longitudinal component of the gust velocity;* θ and $q=\dot{\theta}$ are pitch and pitch-rate, respectively; δ is the control stick input; g is the gravitational constant; and, X_u, M_u, M_q, M_δ are aircraft stability derivatives. The stability derivatives were assumed to have "nominal" values of $X_u=-0.1$, $M_u=0.0207$, $M_q=-3.0$, and $M_\delta=0.431$. We will examine the effects of the variations in these derivatives indicated in table 1 (the case numbers identifying

TABLE 1.—*Variations in VTOL Stability Derivatives*

Case	X_u	M_u	M_q	M_δ
Nominal (PH8)	−0.1	0.0207	−3.0	0.431
PH1	0	0.0207	−3.0	.287
PH2	−.05	0.0207	−3.0	.420
PH5	−.3	0.0207	−3.0	.516
PH6	−.1	0	−3.0	.300
PH7	−.1	.0104	−3.0	.360
PH9	↓	.0312	−3.0	.481
PH10	↓	.0207	−1.0	.369
PH12	↓	.0207	−5.0	.493

the various conditions are those assigned in reference 6).

The pilot was provided with a Norden contact analog display on which both aircraft attitude θ and position x were indicated explicitly. (The display is described in ref. 5.) We assume, on the basis of much evidence, that the pilot is able to infer $\dot{\theta}=q$ and $\dot{x}=u$ from the display, so that the "displayed output" is $y=\text{col}\,\{u,x,q,\theta\}$.

MULTILOOP-MODEL ANALYSIS

A closed-loop pilot-vehicle analysis of the above hover task, using fixed-form, multiloop pilot models was performed by Vinje and Miller. We present the highlights of their approach in an attempt to provide further context for the results we have obtained with our model.*

In applying the multiloop-model approach, one must *assume* an a priori closed-loop system structure. In other words, an assumption must be made concerning those loops "closed" by the pilot. Vinje and Miller assumed the "series loop" model illustrated in figure 2. (A parallel loop model for this task is also a possibility.) Once the loop topology has been decided upon, it is then necessary to assume specific forms for the individual transfers comprising the pilot model. For the structure of figure 2 this means choosing fixed forms for Y_{p_x} and Y_{p_θ}. The forms chosen by Vinje and Miller were

$$Y_{p_x}=K_{p_x}(T_{L_x}s+1)e^{-\tau_x s} \qquad (3)$$

$$Y_{p_\theta}=K_{p_\theta}(T_{L_\theta}s+1)e^{-\tau_\theta s}/(T_N s+1). \qquad (4)$$

In equations (3 and 4), and the "neuromuscular lag" T_N, the θ-loop transport lag τ_θ, and the x-loop transport lag τ_x were considered to be fixed parameters with values of 0.35 sec, 0.09 sec and 0.08 sec, respectively; the gains K_{p_θ}, K_{p_x} and the lead time constants T_{L_θ}, T_{L_x} were assumed to be "adaptable" parameters, chosen by the pilot to achieve certain desired closed-loop characteristics.

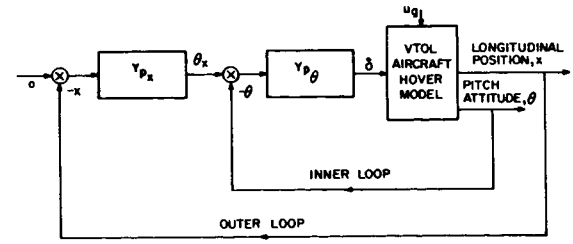

FIGURE 2.—Series loop model for pilot longitudinal control in hover.

* The simulated gust u_g was equivalent to first-order filtered white noise with a bandwidth of 0.314 rad/sec and an rms value of 5.14 ft/sec.

* Details may be found in reference 6.

Inasmuch as Y_{p_x} and Y_{p_θ} cannot be measured directly in this task, Vinje and Miller devised a technique for "identifying" the adaptable parameters. In particular, they iterated on K_{p_θ}, K_{p_x}, T_{L_θ} and T_{L_x} until the rms values σ_u, σ_x, σ_θ, and σ_q computed by using the closed-loop model of figure 2 "matched" the corresponding rms hover performance (as measured in the simulator experiments) to within 0.5 percent. Vinje and Miller did not use rms control activity σ_θ in their matching procedure in an attempt to minimize the effects of ignoring pilot remnant in the computation of the pilot-model adapted parameters. However, they compared measured values of σ_δ with those obtained from calculations based on the computed pilot-model parameters and found that these values of σ_δ differed, on the average, by about 17 percent.

Once values for the parameters of Y_{p_x} and Y_{p_θ} are given, it is possible to compute various loop closure characteristics, e.g., inner- and outer-loop crossover frequencies and phase margins. The inner-loop characteristics are obtained from $Y_{p_\theta}\cdot[\theta/\delta]$. The outer-loop characteristics are calculated by assuming the inner (pitch) loop is closed.

Before leaving this discussion of the multiloop analysis, it is worth repeating and re-emphasizing that the pilot-model adapted parameters and the computed loop closure characteristics are *derived* measures of human performance that are designed to provide additional understanding of the pilot's behavior. The only direct measures made by Vinje and Miller in their experimental study were the measures of closed-loop rms hovering performance σ_x, σ_u, σ_θ, σ_q σ_δ.*

PREDICTIONS WITH THE OPTIMAL CONTROL MODEL

In this section we present the results of applying the optimal control model of the human operator to the analysis of the hover task described earlier. We begin with a brief discussion of the choice of parameters for the optimal control model. Then we present and discuss model predictions for the various configurations listed in table 1.

Model Parameters

Values for τ_N, τ, the ρ_i, and ρ_m as well as cost functional weightings had to be chosen for this task. We felt that, with respect to those parameters related primarily to *intrinsic* human limitations, values representative of those used in the single-axis studies constituted a good a priori choice. Thus, we let $\tau_N = 0.1$ sec, $\tau = 0.15$ sec, $\rho_1 = \rho_2 = \rho_3 = \rho_4 = -20$ dB and $\rho_m = -25$ dB.* It is significant that we were able to keep this (initial) set of model input parameters fixed throughout the entire subsequent study.

The choice of a cost functional is a bit more subtle. Recall that the pilots were instructed to minimize position error σ_x. However, in order to accomplish this the pilot must suppress pitch errors inasmuch as such errors introduce disturbing longitudinal forces. In addition, one may expect that pilots try to avoid excessive attitude changes during the process of minimizing hovering errors. Accordingly, it seems reasonable to include a pitch or pitch-rate term in the cost functional; we chose to add a term proportional to mean-squared pitch rate, σ_q^2. We picked the pitch-rate weighting on the basis of the measured scores for the "nominal" configuration.† In that case, values of σ_x^2 and σ_q^2 of approximately 1.2 ft^2 and 0.0024 rad^2/sec^2 were found. On this basis, we selected a pitch-rate weighting of 400 and we used this value in all subsequent calculations. Thus, the cost functional for this analysis was

$$J = \sigma_x^2 + 400\sigma_q^2 + g\sigma_\delta^2 \tag{5}$$

where g was chosen so that $\tau_N \simeq 0.1$ sec.

Nonimal Case

We now compare model predictions with measured and derived data for the nominal case (PH8 in table 1). Measured and predicted scores are compared below in table 2. The measured

* Another (subjective) measure, namely, pilot opinion rating was also taken but we will not discuss this measure at length here.

* Noise ratios were chosen within ± 0.5 dB and τ_N was within 10 percent of 0.1 sec for all cases.

† Other, a priori, techniques for choosing the weighting are possible.

TABLE 2.—*Comparison of Measured and Predicted Scores for Nominal Configuration* ($X_u = -0.1$, $M_u g = 0.667$, $M_q = -3$, $M_\delta = 0.431$)

	σ_u	σ_x	σ_q	σ_θ	σ_δ
Measured	0.79(0.09)	1.16(0.10)	0.050(0.003)	0.032(0.002)	0.59(0.03)
Predicted	.82	1.08	.055	.036	.63

values are averages of ten runs and the quantities in parenthesis indicate the corresponding standard deviations. It can be seen that the agreement between predicted and measured scores is excellent.*

It would be desirable to obtain comparisons of measured and predicted frequency domain data for this study that might provide a more complete validation of the model. Unfortunately, the data of reference 6 does not include frequency domain measurements. Instead, the fixed-form expressions for Y_{p_x} and Y_{p_θ} were assumed and the parameter values (K_{p_θ}, K_{p_x}, T_{L_θ}, T_{L_x}) were adjusted to match scores.

In an attempt to correlate the multi-loop structure of our optimal-control-model with that of Vinje and Miller's model, we simply computed the equivalent transfers, Y_{p_θ} and Y_{p_x} in the following manner. From figure 2, we see that the control input

$$\delta = -Y_{p_x} Y_{p_\theta} x - Y_{p_\theta} \theta. \tag{6}$$

On the other hand, for this situation, we may write the output of the optimal control model of the human operator as (see ref. 1 and Fig. 1)

$$\begin{aligned}\delta(s) = \underline{h}'\underline{y} &= h_1(s)u(s) + h_2(s)x(s) + h_3(s)q(s) \\ &\quad + h_4(s)\theta(s) \\ &= (sh_1 + h_2)x(s) + (sh_3) + h_4)\theta(s)\end{aligned} \tag{7}$$

Comparison of equations (6) and (7) yields

$$sh_3 + h_4 = -Y_{p_\theta} \tag{8}$$

$$\frac{sh_1 + h_2}{sh_3 + h_4} = Y_{p_x}. \tag{9}$$

Consequently, with these expressions for Y_{p_θ} and Y_{p_x}, it is possible to use the optimal control model to compute equivalent "inner" and "outer" loop characteristics, just as is done in the fixed-form multiloop analysis.

Figures 3 through 5 show the results of performing some of the frequency domain calculations for the "nominal" configuration. Bode plots

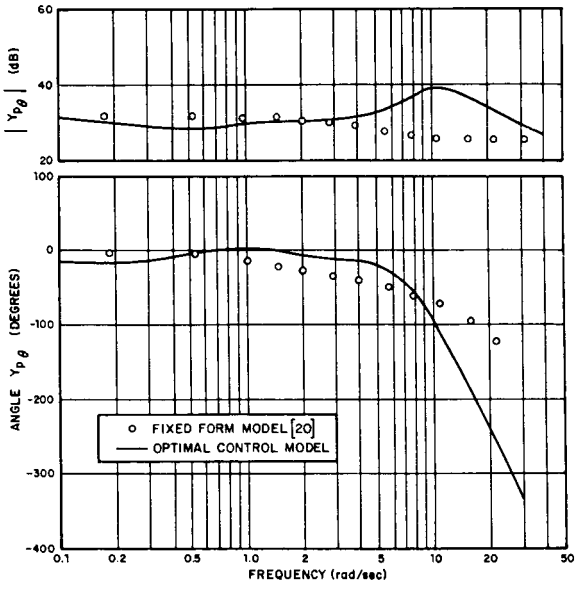

FIGURE 3.—Pitch-loop pilot describing functions Y_{p_θ} for nominal configuration.

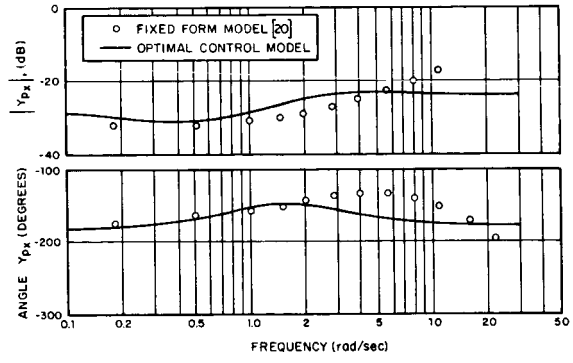

FIGURE 4.—Position-loop pilot describing functions for nominal configuration.

* It should be emphasized the only "parameter" used to "match" this data was the pitch-rate weighting.

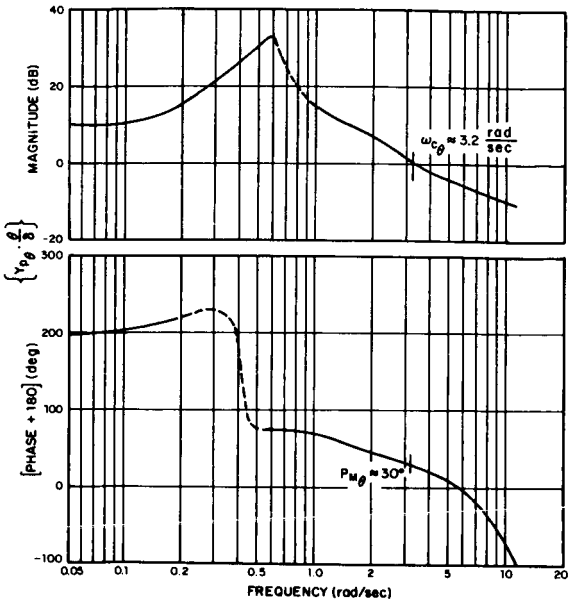

FIGURE 5.—Open loop describing function for pitch loop, $\{Y_{p_\theta} \cdot \theta/\delta\}$.

of Y_{p_θ} and Y_{p_z}, as computed from equations (8) and (9), are presented in figures 3 and 4. Also shown in these figures are the fixed-form Y_{p_θ} and Y_{p_z} corresponding to the parameter values (K_{p_θ}, T_{L_θ}, K_{p_z}, etc.) determined by Vinje and Miller. As can be seen, the corresponding Y_{p_θ}-transfers are in excellent agreement up to about 4 rad/sec; correspondingly good agreement between the Y_{p_z}-transfers is evident up to about 1.5 rad/sec.

In figure 5, the Bode plots for the transfer $\{Y_{p_\theta} \cdot \theta/\delta\}$, necessary to determine "inner"-loop closure characteristics, is presented.* We find that the optimal control model yields, for the pitch loop, "crossover" frequency and phase margin of approximately 3.2 rad/sec and 30°, respectively. Vinje and Miller obtain a pitch loop crossover frequency and phase margin of 3.1 rad/sec and 8°. Similar computations for the "outer" or position loop result in model crossover and phase margin of 1.1 rad/sec and 21° as compared to values of 1.0 rad/sec and 15° derived by Vinje and Miller. Thus, the agreement in these characteristics is good, with the optimal control model providing slightly greater stability margins.

The loop closure characteristics reveal that the Y_{p_θ} and Y_{p_z} predicted by the optimal control model agree closely with the derived values of Vinje and Miller up to frequencies slightly greater than the respective loop crossovers. The disagreements at higher frequencies cannot be resolved on the bais of the available data and they do not appear to be significant from the standpoint of system performance. However, from our studies of single-axis tasks, we can be reasonably certain that the high frequency deviations of the Y_p result from the longer time delay and the inclusion of the predictor in the optimal-control model.

Effects of Pitch Rate Damping, M_q

Predicted and measured rms-scores as a function of changes in pitch rate damping (with other derivatives held at "nominal" values) are plotted in figure 6. It should be re-emphasized that no changes in the parameters of the pilot model are made in computing the effects of changing aircraft parameters. Again, agreement is quite good, especially for the cases with higher damping. For $M_q = -5.0$, all the predicted scores are within the standard deviations of the data and we have already seen similar agreement for the $M_q = -3.0$ case. Model predictions are poorest for the configuration with the least damping ($M_q = -1.0$), although the maximum deviation between predicted and measured scores does not exceed 25 percent. Unfortunately, it is difficult to assess the true mismatch between model scores and data for this case because standard deviations of the measured averages were not available. (Standard deviations were published for the results of a second, different, subject; as might be expected, standard deviations increased as damping decreased.)

What is perhaps most surprising about the score data for the low damping case is that all the scores predicted by the optimal-control model of the human operator *exceed* those achieved by the pilot. This suggests that the observation noise-ratios in the model may have been too high. We

* The dashed portions of these curves correspond to what we believe are reasonable trends in the data. Unfortunately, our programs were designed to compute quantities at discrete frequencies (corresponding to values at which we normally measure). Time did not permit the recomputations necessary to define these frequency plots in more detail.

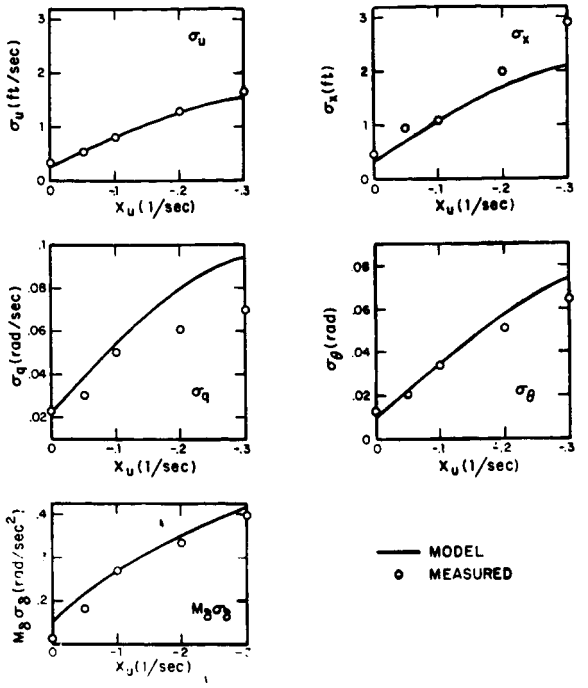

FIGURE 6.—Effect of pitch-rate damping on hovering performance ($M_u g = 0.667$, $X_u = -0.1$).

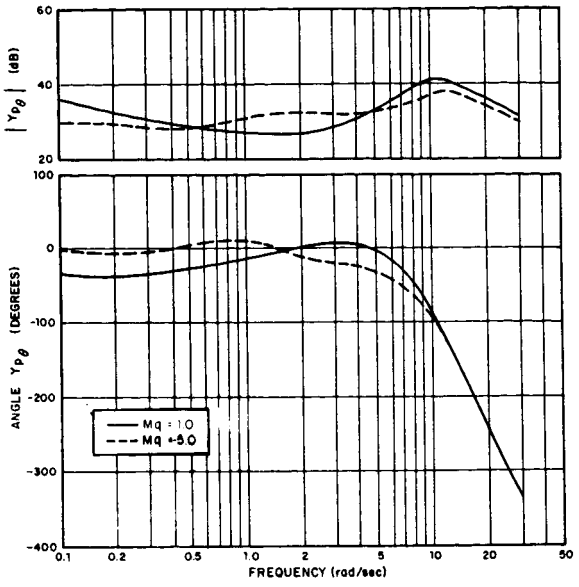

FIGURE 7.—Effect of pitch rate damping on predicted pilot describing function for pitch loop ($M_u g = 0.667$, $X_u = -0.1$).

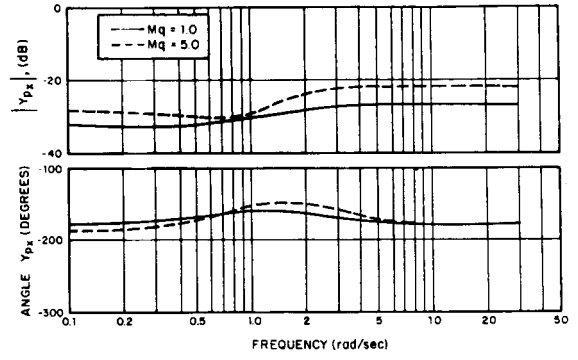

FIGURE 8.—Effect of pitch rate damping on predicted pilot describing function for position loop ($M_u g = 0.667$, $X_u = -0.1$).

decreased these noise-ratios to approximately −23 dB and found that *all* predicted scores were then within 10 percent of measured values. This is an interesting result because it implies that the pilots became less "random," in an attempt to maintain the lower scores. Or, in Levison's (ref. 7) terms, the pilots worked harder to achieve a criterion level. This correlates with the fact that the $M_q = -1.0$ case was rated unsatisfactory by the pilots (ref. 6) whereas the cases with higher damping were rated satisfactory.

The equivalent Y_{p_θ} and Y_{p_x} obtained from the optimal control model are plotted in figures 7 and 8. Naturally, the simplified fixed-form expressions of reference 6 will not duplicate the low-frequency variations seen in the Y_{p_θ} transfer with $M_q = -1.0$. Nor will the high frequency behavior of corresponding transfers be duplicated for the reason mentioned earlier. However, it can be verified that in the neighborhood of crossover, both models yield pitch and position loop gains that agree quite well. Thus, we found inner and outer loop crossover frequencies that agreed with those of reference 21 to within plotting accuracies.

Effects of Speed Stability Parameter, M_u

The effects on predicted and measured scores of changing the speed stability parameter M_u are shown in figure 9. The agreement is again very good except for the smallest value of $M_u = 0$. The less precise agreement for the $M_u = 0$ case is probably attributable to a value of motor noise that is too small. In this case there is no gust component entering in parallel with the stick so the Kalman filter can obtain very good estimates

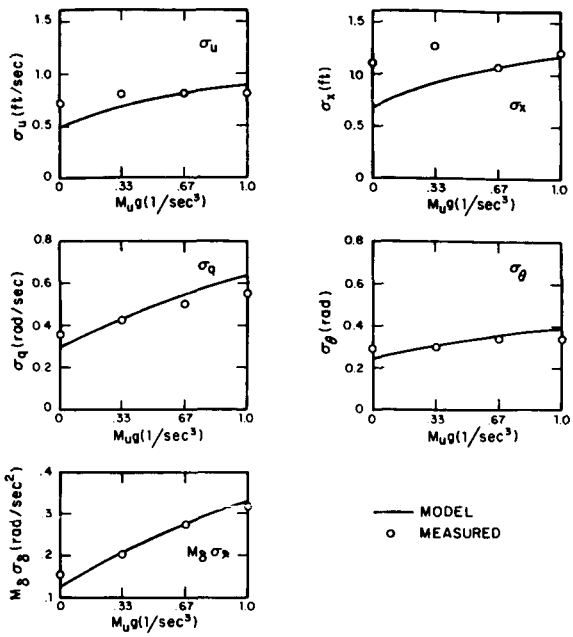

FIGURE 9.—Effect of speed stability parameter on hovering performance ($Mq = -3.0$, $X_u = -0.1$).

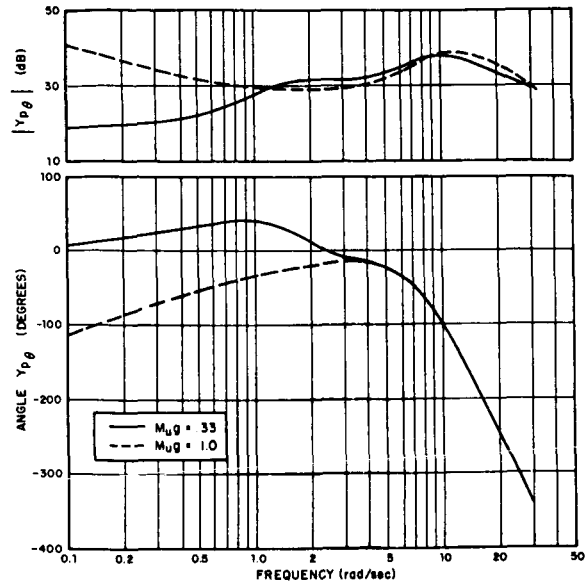

FIGURE 10.—Effect of speed stability parameter on predicted pilot describing function for pitch loop ($Mq = -3.0$, $X_u = -0.1$).

of q and θ. We have found in a previous study (ref. 3), that such a situation may require values of motor noise somewhat greater than -25 dB to model the human operator accurately.*

Equivalent Y_{p_θ} and Y_{p_x} transfers for the cases $M_u g = 0.33$ and $M_u g = 1.0$ are shown in figures 10 and 11. Variations in Y_{p_θ} with $M_u g$ take place almost entirely below 1 rad/sec. (The nominal Y_{p_θ} for $M_u g = 0.667$ falls within those shown.) In the neighborhood of pitch loop crossover ($\sim$3 rad/sec), pitch loop gain decreases very slightly with increasing $M_u g$. This was also true for the fixed-form model of reference 6. The variations in Y_{p_x} (fig. 11) with $M_u g$ are not very dramatic, with relatively small changes in gain appearing to be the principal effect. It should be noted that the position gain of the optimal control model decreases with increasing $M_u g$, whereas the K_{p_x} of the fixed-form model shows the opposite trend. However, the total variation in position loop gain for the fixed-form model is less than 2 dB and the observed trend may not be significant.

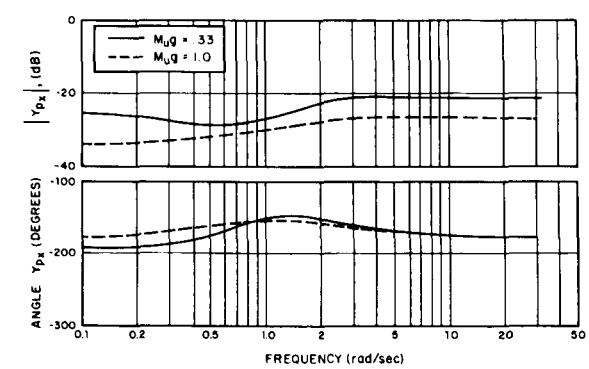

FIGURE 11.—Effect of speed stability parameter on predicted pilot describing function for position loop ($Mq = -3.0$, $X_u = -0.1$).

Effects of Variations in Longitudinal Drag Parameter, X_u

Predicted scores were computed for various values of X_u (with M_q and $M_u g$ kept at their nominal values) and are presented along with measured data in figure 12.* Again, the data

* Note that moderately higher values of motor noise would not increase the scores significantly in the remaining cases examined in this paper because of the relatively large nominal value for $M_u g$.

* Frequency domain data were also computed but they evidenced similar phenomena as in the other cases and are therefore not presented.

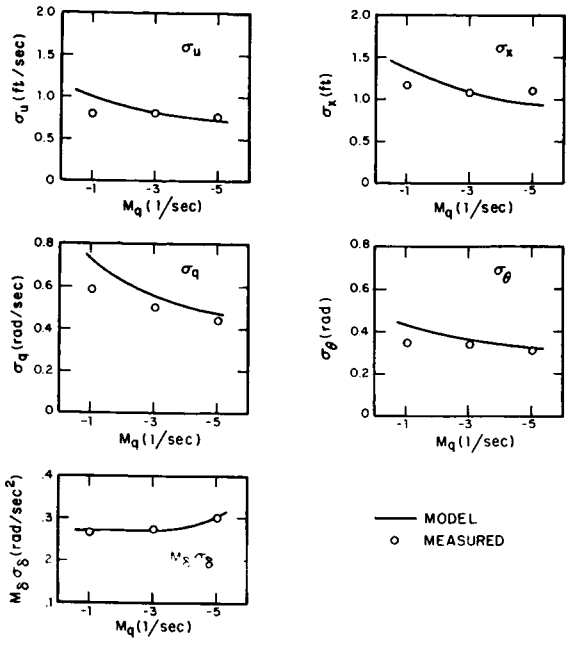

FIGURE 12.—Effect of longitudinal drag parameter on hovering performance ($M_u g = 0.667$, $Mq = -3.0$).

agree almost everywhere; major trends are reproduced and actual values are in close agreement. The only exception is the $X_u = -0.3$ case where the model predicts lower position, and higher pitch scores than were actually measured.

Predicted and measured scores could be brought in closer agreement for $X_u = -0.3$ by increasing the pitch rate weighting. We therefore obtained model predictions for a weighting of $q_4 = 1000$, a two and one-half-fold increase. The results, along with the measured values and those obtained with the lower weighting, are presented in table 3. (Numbers in parentheses are standard deviations.) Thus, it would appear from these results that the pilot was unwilling to accept the higher pitch-rate scores associated with the larger turbulence (X_u multiplies the input) * and increased his pitch-rate weighting accordingly. It is interesting to note that this configuration had the poorest pilot rating of all the cases that we investigated.

SUMMARY AND CONCLUDING REMARKS

We have applied the optimal control model of the human operator to predict performance in a series of longitudinal hovering tasks. The configurational changes that were considered significantly altered the system response to both control and disturbance inputs, yet the model was able to predict performance with exceptional accuracy in almost all cases. Moreover, this was accomplished with a fixed set of model input parameters, whose values were virtually identical to those used in single-axis studies. Also needed in the analysis was a subjective" weighting on rms pitch-rate error (i.e., a measure of performance in the "additional loop"). Results for all but one case were quite good keeping this parameter invariant and reasonable methods for selecting its value appear to be generally available.

Inasmuch as no frequency domain measurements were available for comparison, the optimal control model was used to predict describing functions that corresponded to the "loop closing" pilot transfer functions that are frequently employed in "classical" multiloop manual control analyses. These "equivalent-optimal" describing functions were compared with fixed-form transfer functions that had been derived in the original analyses of the data. The fixed-form transfer

* Vinje and Miller also draw the same inference from their data.

TABLE 3.—*Score Comparison for Different Pitch-Rate Weightings in High Drag Configuration*

	σ_u	σ_x	σ_q	σ_θ	σ_δ
Measured	1.67(0.20)	2.88(0.45)	0.069(0.005)	0.064(0.005)	0.76(0.07)
$q_4 = 400$	1.58	2.10	.095	.074	.82
$q_4 = 1000$	1.66	2.52	.079	.070	.68

functions were of the "crossover-model" genre, and had some preselected parameters (time delays and neuromotor time constant) and some parameters (gain and lead time constants) that were adjusted to match measured score data.

Invariably, the optimal control and fixed-form describing functions agreed quite well in the neighborhood of loop "crossovers." This is not surprising because the optimal control model predicts the measured scores and the fixed-form model, which is designed primarily for the crossover region, is adjusted to match the "same" measured scores. For frequencies outside the crossover range, agreement between the differently obtained describing functions is generally not good. This is particularly evident for pitch-loop pilot describing functions. Those describing functions obtained from the optimal control model exhibit much more complex behavior than do the simpler fixed-form transfers. Many of these complex response characteristics are quite similar to those predicted by the model, and also observed experimentally, in single-axis tasks. On this basis we believe that measured describing functions would bear a closer resemblance to those predicted by the optimal control model than to those obtained from the fixed-form model with "measured" parameters.

There were three cases for which the optimal control model did not yield very accurate score predictions. For one of these cases ($M_u g = 0$) the discrepancies could be largely attributed to our treatment of motor noise. In the other two cases, more accurate predictions were achieved by changing model input parameters. In one case (lowest pitch rate damping), the observation noise ratio was decreased, and in the other case (highest drag) the pitch-rate weighting was increased. It is interesting and important to note that both of these cases were ones in which significantly poorer pilot ratings were obtained. It would appear to be more than coincidental that a change in the basic model parameters correlated with a substantial degradation in pilot rating. Although, much work remains to be done, we are reasonably convinced that the optimal control model will ultimately provide a versatile and fairly general approach to predicting aircraft flying qualities.

REFERENCES

1. KLEINMAN, D. L.; AND BARON, S.: Manned Vehicle Systems Analysis by Means of Modern Control Theory. Rept. No. 1967, Bolt Beranek and Newman Inc., June 1970.
2. KLEINMAN, D. L.; BARON, S.; AND LEVISON, W. H.: An Optimal Control Model of Human Response. Part I: Theory and Validation. Automatica, vol. 6, no. 3, May 1970.
3. BARON, S.; KLEINMAN, D. L.; ET AL.: Application of Optimal Control Theory to the Prediction of Human Performance in a Complex Task. AFFDL–TR–69–81, Wright-Patterson Air Force Base, Mar. 1970.
4. KLEINMAN, D. L.; AND BARON, S.: Analytic Evaluation of Display Requirements for Approach to Landing. Rept. No. 2075, Bolt Beranek and Newman Inc., Mar. 1971.
5. VINJE, E. W.: AND MILLER, D. P.: Interpretation of Pilot Opinion by Application of Multiloop Models to a VTOL Flight Simulator Task. NASA SP–144, Mar. 1967.
6. MILLER, D. P.; AND VINJE, E. W.: Fixed-Base Flight Simulator Studies of VTOL Aircraft Handling Qualities in Hovering and Low-Speed Flight. AFFDL–TR–67–152, Wright-Patterson Air Force Base, Jan. 1968.
7. LEVISON, W. H.; ELKIND, J. I.; AND WARD, J. L.: Studies of Multivariable Manual Control Systems: A Model for Task Interference. Rept. No. 1892, Bolt Beranek and Newman Inc., Dec. 1969. Also NASA CR–1746.